Numerical Investigation of Diameter Effects on the Cyclic and Axial Behavior of Spun Piles

Muh. Ricki Saprollah[1], Ali Awaludin[1]*, Angga Fajar Setiawan[1]
[1]Department of Civil and Environmental Engineering, Gadjah Mada University, Yogyakarta, INDONESIA
**Corresponding author:* ali.awaludin@ugm.ac.id

ABSTRACT

Prestressed spun piles are widely used in deep foundation systems due to their high capacity to withstand combined axial and lateral seismic loads. Ensuring reliable performance under cyclic loading is essential for the safety and resilience of structures in earthquake-prone areas. This study presents a comprehensive numerical investigation on the cyclic behavior of prestressed spun piles with diameters of 400 mm, 500 mm, and 600 mm, considering both hollow and reinforced concrete infill configurations. A total of eighteen models were developed, incorporating reinforcement ratios of 1% and 2% in the infilled piles. Axial loads were applied at two levels, $0.08f_c'A_g$ and $0.16f_c'A_g$, while lateral cyclic displacements were imposed following the ACI 374.1-05 protocol to simulate realistic seismic demands. Nonlinear structural responses were captured using fiber-section beam-column modeling techniques, calibrated against experimental data for validation. The results show that increasing pile diameter enhances the ultimate moment capacity, while only infill piles achieve a significant improvement in ductility. The findings offer valuable insights for optimizing the seismic design of prestressed spun piles.

Keywords: Spun piles, Cyclic behavior, Diameter, Fiber-section, Nonlinear.

1 INTRODUCTION

Prestressed spun piles have become a preferred option for deep foundation systems, particularly in seismically active areas. Their widespread use is driven by a combination of structural and practical advantages, including a high strength-to-weight ratio, ease of prefabrication and installation, as well as economic efficiency. These characteristics make spun piles especially suitable for supporting both vertical and lateral loads in critical infrastructure such as bridges, port structures, and elevated roadways where seismic resilience is essential.

Despite their benefits, the structural response of prestressed spun piles under cyclic lateral loading remains an important subject of investigation. Although prestressing enhances flexural strength and cracking resistance, concerns persist regarding potential inelastic deformations, localized damage, and degradation of stiffness during seismic events. As highlighted by Ren et al. (2022), spun piles generally perform well under cyclic loading but still exhibit vulnerabilities under large displacement demands.

Experimental studies have provided valuable insights into these behaviors. Irawan et al. (2018) examined hollow spun piles with a diameter of 400 mm subjected to combined axial and lateral cyclic loading. The results showed a peak lateral resistance of approximately 290 kN and a displacement ductility of around 2.60. While the pile demonstrated adequate initial stiffness, the limited ductility raises concerns about its performance under strong ground motion scenarios.

In parallel with experimental approaches, numerical modeling has become increasingly important in analyzing the seismic behavior of spun piles. Setiawan et al. (2020) utilized a fiber-section model employing *Concrete07* for concrete and *Steel02* for reinforcement to simulate the behavior of prestressed hollow concrete piles. The simulation results showed good agreement with experimental data, with deviations of approximately 12.5 percent for yield and ultimate lateral capacities. This validated the reliability of the model in capturing essential features of cyclic behavior.

Understanding the nonlinear response of spun piles under seismic loading is critical for performance-based design, particularly in preventing brittle failure and ensuring structural safety. Irawan et al. (2020) emphasized that accurate knowledge of deformation mechanisms and energy dissipation is necessary for enhancing ductility and resilience. Nevertheless, there remains a significant research gap concerning the influence of geometric parameters, especially pile diameter, on seismic performance.

Previous studies have primarily focused on variables such as axial load levels, prestressing effects, and section configurations, including hollow and concrete-filled piles (Darmawan et al., 2024; Setiawan et al., 2023; and Ren et al., 2022). However, systematic investigations that isolate pile diameter as an independent parameter remain limited. Most previous experimental and numerical investigations, including the work by Fajar et al. (2020), generally adopted a single pile diameter across multiple test conditions, which restricts the isolation of diameter-specific influence on performance.

Furthermore, although numerous studies have addressed the interaction between axial and lateral loads under cyclic conditions (Owji et al., 2024; Hu et al., 2019; and Li et al., 2010), the influence of pile diameter on displacement-based responses, such as ductility and stiffness degradation, has received comparatively less attention. This gap in understanding size-dependent effects highlights a critical limitation in current performance-based design recommendations.

To fill this research gap, the present study conducts a numerical investigation on prestressed spun piles with diameters of 400 mm, 500 mm, and 600 mm. Each pile model is subjected to axial loads of 0.08 $f_c'A_g$ and 0.16 $f_c'A_g$, where f_c' is the concrete compressive strength and A_g is the gross cross-sectional area, along with lateral reversed cyclic displacement loading following the ACI 374.1-05 protocol (Irawan et al., 2018). The main objectives are to evaluate how diameter variation affects key performance indicators such as lateral load capacity and displacement ductility, and to validate the accuracy of numerical simulations by comparing the results with established experimental data.

2 METHODS

2.1 Geometric and Material Nonlinearity

The spun piles were modeled using nonlinear beam-column elements with fiber section definitions to accurately capture the distribution of plasticity across the cross-section (Setiawan et al., 2020). Concrete was modeled using the *Concrete02* material model, which incorporates compressive softening, tensile cracking, and stiffness degradation. The stress–strain relationship was based on the modified Kent and Park (1971) model.

To improve accuracy, tensile properties dependent on compressive strength (f_c') and the initial elastic modulus (E_0) were included, following the approach by Quayyum (2010). Steel reinforcement was modeled using the *Steel01* material, which exhibits bilinear behavior with both kinematic and isotropic hardening, suitable for reversed cyclic loading conditions. Geometric nonlinearity, including P-Delta effects and large displacements, was captured using a *corotational* transformation.

2.2 Material Properties and Parameters

Table 1 summarizes the key material properties adopted from Irawan et al. (2018). These parameters are critical for capturing the nonlinear behavior of spun piles under combined axial and cyclic loading. The values reflect standardized properties of concrete and prestressed steel reinforcement, contributing to the robustness and reliability of the analysis. Table 2 summarizes the material properties of the reinforced concrete infill, which consists of concrete with a compressive strength of 33 MPa and steel reinforcement with a yield strength of 400 MPa.

Table 1. Material properties and parameters of prestressed spun piles.

Material	Parameter	Value	Description
Concrete (*Concrete02*)	f_c'	54.4 MPa	Concrete compressive strength at 28 days
	e_{psc0}	–0.002	Concrete strain at maximum strength
	f_{pcu}	–10.88 MPa	Concrete crushing strength
	e_{psU}	–0.00316	Concrete strain at crushing strength
	λ	0.071	Curve parameter for concrete
	f_t	4.425 MPa	Tensile strength
	E_{ts}	54400 MPa	Tension softening stiffness
	Initial Stress	–4.6 MPa	Prestress in concrete
PC-Bar (*Steel01*)	f_y	1387 MPa	Yield strength
	E_0	220267 MPa	Initial elastic tangent
	b	0.01989	Strain-hardening ratio
	ε_{min}	–0.018	Minimum value of strain
	ε_{max}	0.018	Maximum value of strain
	Initial Stress	1095 MPa	Initial stress in PC bar

Table 2. Material properties and parameters of reinforced concrete infill.

Material	Parameter	Value	Description
Concrete infill (*Concrete02*)	f_c'	33 MPa	Concrete compressive strength at 28 days
	e_{psc0}	–0.002	Concrete strain at maximum strength
	f_{pcu}	–6.6 MPa	Concrete crushing strength
	e_{psU}	–0.00505	Concrete strain at crushing strength
	λ	0.1	Curve parameter for concrete
	f_t	3.447 MPa	Tensile strength
	E_{ts}	33000 MPa	Tension softening stiffness
Steel reinforcement (*Steel01*)	f_y	400 MPa	Yield strength of steel reinforcement
	E_0	200000 MPa	Initial elastic tangent

2.3 Model Configuration

This study numerically analyzes 18 prestressed spun pile models with diameters of 400 mm, 500 mm, and 600 mm, considering both hollow and reinforced concrete infill configurations. All piles have a uniform wall thickness of 100 mm and a prestressing strand ratio of 0.45%, as illustrated in Figure 1. The model was developed to simulate the behavior of spun piles subjected to combined axial and cyclic lateral loading.

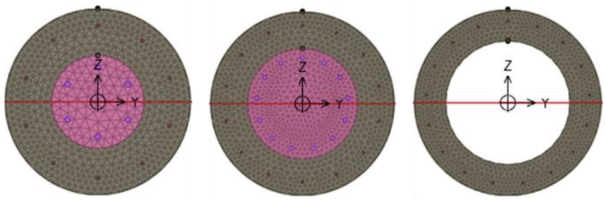

(a) (b) (c)

Figure 1. Models of prestressed spun piles (a) 400 mm, (b) 500 mm, and (c) 600 mm.

2.4 Idealization of the Numerical Model

In this study, the idealization of the spun pile structure was based on the experimental setup by Irawan et al. (2018) and was modeled using the STKO pre-processor for OpenSees. The numerical model does not incorporate soil–structure interaction. A perfect bond is also assumed between the reinforcement and the concrete. Furthermore, a single cyclic loading protocol is adopted, which may not fully represent all earthquake scenarios.

The spun pile structure consists of five nodes, three lines, and two interactions, as illustrated in Figure 2. The pinned support restrains translation in the UX, UY, and UZ directions as well as rotation about the RZ axis. The roller support restrains translation in the UX and UY directions and rotation about RZ. A dummy node is assigned as the control point for the application of cyclic lateral loading. This node is restrained in all degrees of freedom (DOFs) except for translation in the UX direction.

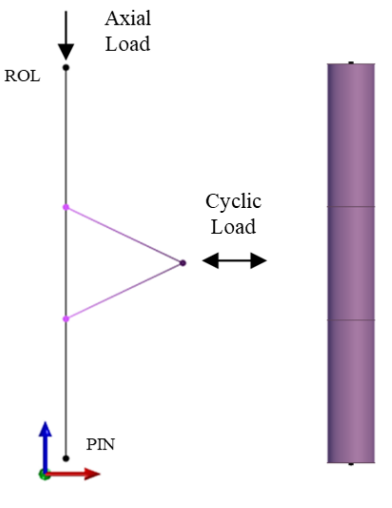

Figure 2. Loading protocol in OpenSees.

All pile models were assigned a uniform span length of 3500 mm, in accordance with the experimental setup by Irawan et al. (2018). This constant length served as a control variable to isolate the effects of diameter and other parameters, ensuring that observed variations in structural performance were not influenced by differences in member length. Based on this configuration, the applied cyclic loading pattern is illustrated in Figure 3.

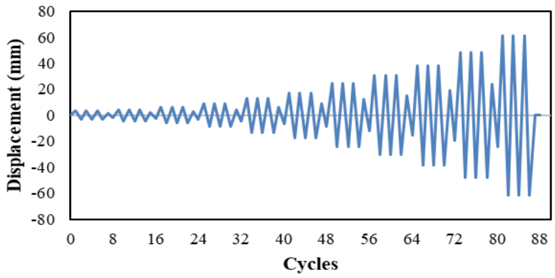

Figure 3. Cyclic load.

2.5 Validation with Experimental Data

In the experimental setup (Irawan et al., 2018), the pile was subjected to an axial load of 0.16 $f_c'A_g$, simulating the service-level axial force. Subsequently, lateral cyclic displacement was applied following a displacement-controlled loading protocol divided into three ductility levels (μ_1, μ_2, μ_3) to capture the progressive nonlinear behavior under increasing deformation demands. The hysteresis curves shown in Figure 4 confirm the numerical model's accuracy, as the simulated curve closely follows the experimental.

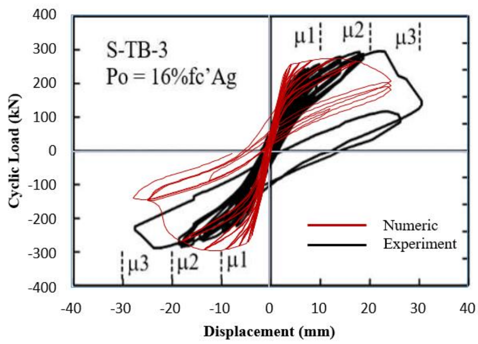

Figure 4. Comparison between experimental and numerical

The experiment recorded an ultimate moment capacity of 160.00 kN·m, while the numerical prediction was slightly lower at 155.39 kN·m, corresponding to a deviation of 2.88%. This close match demonstrates the model's ability to accurately replicate the nonlinear flexural response of the reinforced concrete infill spun pile under cyclic lateral loading. The ductility obtained from the experiment was 2.40, while the numerical simulation yielded a value of 2.94, indicating a relatively small deviation (13.08%). Therefore, the developed numerical model can be reliably used for further parametric studies.

3 RESULT AND DISCUSSION

3.1 Lateral Load–Displacement Response

A comparative parametric study was conducted on eighteen prestressed spun pile specimens with diameters of 400 mm, 500 mm, and 600 mm, consisting of both hollow sections and reinforced concrete infill (f_c' = 33 MPa). The lateral displacement–load responses for the hollow piles subjected to an axial load of 0.16 $f_c'A_g$ are illustrated in Figure 5. As observed, increasing the pile diameter generally resulted in a higher ultimate moment capacity, attributed to the greater flexural stiffness and moment of inertia. However, this strength gain was accompanied by a noticeable reduction in ductility, indicating a trade-off between flexural capacity and deformation ability in hollow configurations. Figure 6 presents the displacement–load curves for the reinforced concrete infill specimens under a lower axial load of 0.08 $f_c'A_g$. Similar to the hollow sections, the ultimate moment exhibited a positive correlation with increasing diameter. Nonetheless, the ductility response was less consistent. Although the infilled piles, on average, outperformed the hollow sections in terms of ductility due to improved confinement and greater energy dissipation provided by the concrete core, certain configurations exhibited slightly lower ductility values compared to their hollow counterparts.

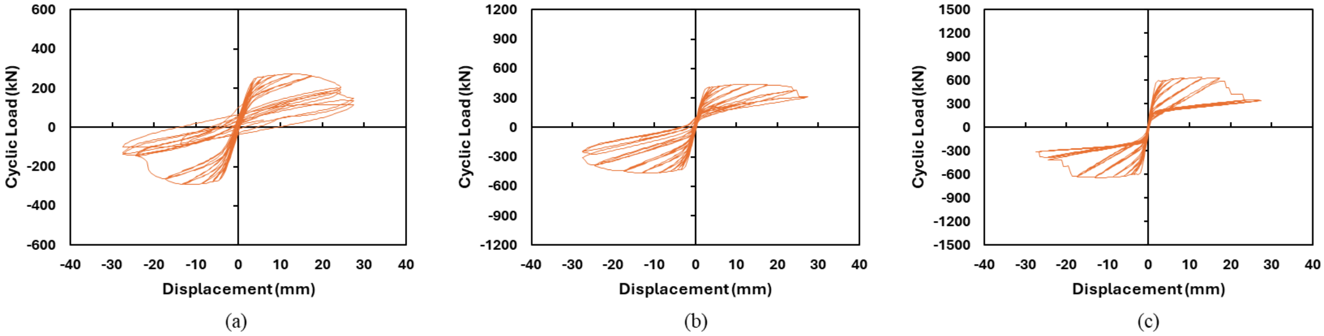

Figure 5. Lateral load–displacement curve of hollow spun piles (a) 400 mm, (b) 500 mm, and (c) 600 mm.

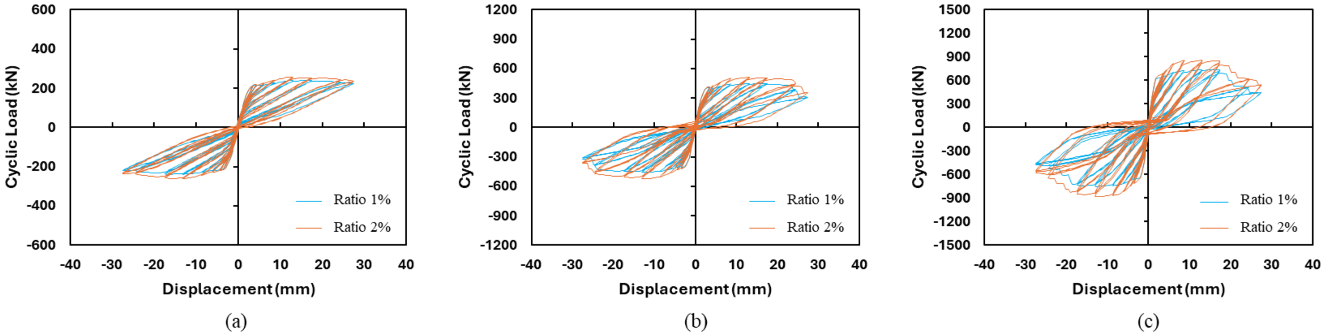

Figure 6. Lateral load–displacement curve of reinforced concrete infill spun piles (a) 400 mm, (b) 500 mm, and (c) 600 mm.

These findings highlight that while increasing diameter and incorporating reinforced concrete infill are generally effective strategies for enhancing ultimate moment capacity, their influence on ductility is more nuanced and may not follow a uniform trend. Accordingly, axial load level, reinforcement ratio, and cross-sectional configuration must be considered holistically in the seismic design of spun piles. The corresponding ductility and ultimate moment values for all eighteen numerical models are summarized in Table 3, providing a comprehensive overview of the structural performance trends discussed above.

Table 3. Ductility and ultimate moment of spun piles

Type	f_c' (MPa)	Reinforcement ratio (%)	Axial load	Ductility (μ)			Ultimate moment (kN.m)		
				400 mm	500 mm	600 mm	400 mm	500 mm	600 mm
Hollow	-	-	0.08 $f_c'A_g$	4.77	4.12	3.91	135.05	221.84	316.47
			0.16 $f_c'A_g$	2.94	3.91	3.75	169.96	275.42	398.46
Infill	33	1	0.08 $f_c'A_g$	5.04	6.38	6.27	149.24	279.18	459.95
			0.16 $f_c'A_g$	4.68	4.06	4.47	183.69	342.51	554.13
		2	0.08 $f_c'A_g$	5.17	6.53	6.60	160.95	319.89	535.85
			0.16 $f_c'A_g$	4.79	4.22	4.81	192.30	377.08	625.61

3.2 Effect of Diameter on Ductility and Ultimate Moment

Increasing the diameter consistently enhances the ultimate moment capacity. For example, under 0.08 $f_c'A_g$ axial load, the moment increased by over 130% from 400 mm to 600 mm. The effect is even more significant with 2% reinforcement and higher axial loads, showing an increase of over 225%. In contrast, ductility does not always improve with larger diameters. In hollow piles, ductility decreases, highlighting the lack of confinement. Infill piles tend to show higher ductility with increasing diameter, particularly under lower axial loads. These findings indicate that larger diameters are effective in enhancing flexural strength, but ductility optimization depends strongly on section configuration and axial loading.

3.3 Influence of reinforced concrete infill

The introduction of reinforced concrete infill significantly improved both ductility and ultimate moment capacity compared to hollow piles. At 400 mm diameter under 0.08 $f_c'A_g$ axial load, ductility increased from 4.77 (hollow) to 5.04 and 5.17 for 1% and 2% reinforcement ratios, respectively. At 600 mm diameter, the increase was even more substantial: from 3.91 (hollow) to 6.27 (reinforced concrete infill with 1% reinforcement) and 6.60 (reinforced concrete infill with 2% reinforcement), indicating a ductility enhancement of approximately 60–69%. Similarly, ultimate moment capacity for 600 mm piles under 0.08 $f_c'A_g$ increased from 316.47 kN·m (hollow) to 535.85 kN·m (reinforced concrete infill with 2% reinforcement), a gain of nearly 70%. These performance enhancements are attributed to the concrete core, which provides confinement and stiffness, thereby delaying local buckling and improving load distribution across the section. This observation aligns with experimental findings by Setiawan et al. (2020) and Irawan et al. (2020), who reported improved structural performance in reinforced concrete infill tubular piles under cyclic loading.

3.4 Interaction of Axial Load and Reinforcement Ratio

Under higher axial load (0.16 $f_c'A_g$), hollow piles generally exhibited a reduction in ductility, likely due to increased axial compression limiting lateral deformation. However, infill piles with higher reinforcement ratios were able to maintain or even improve ductility. At 600 mm diameter, increasing the reinforcement ratio from 1% to 2% resulted in an increase in ductility from 4.47 to 4.81, and an increase in ultimate moment from 554.13 kN·m to 625.61 kN·m (a 13% improvement). These findings suggest that reinforced concrete infill and higher reinforcement ratios can offset the negative impact of high axial loads by enhancing flexural strength and energy dissipation capacity.

4 CONCLUSION

Increasing the pile diameter significantly enhances ultimate moment capacity. However, in hollow sections, this may lead to reduced ductility as a result of limited confinement, which can accelerate local buckling. Incorporating reinforced concrete infill addresses this issue by improving confinement and delaying local buckling, thereby enhancing both ductility and post-yield behavior. Furthermore, higher reinforcement ratios in infill piles help counteract the adverse effects of increased axial load, contributing to improved seismic performance overall.

ACKNOWLEDGEMENTS

The authors would like to express their deepest gratitude to the Education Fund Management Institute (LPDP – Indonesia Endowment Fund for Education), under the Ministry of Finance of the Republic of Indonesia, for supporting this research and its publication.

REFERENCES

Darmawan, M. F., Setiawan, A. F., Satyarno, I., & Awaludin, A. (2024). Nonlinear simulations to evaluate the code-based response modification factor for seismic design of slab-on-pile structure. *ASEAN Engineering Journal*. Published online February 29, 2024.

Fajar, A. S., Darmawan, M. F., Yogatama, B. A., Satyarno, I., & Guntara, M. (2020, September 13–18). *Seismic performance investigation of bracing and SPD application in PHC pile as viaduct piers* [Paper presentation]. 17th World Conference on Earthquake Engineering (17WCEE), Sendai, Japan.

Hu, K., Su, D., Yu, Z.-L., Huang, J.-J., & Pang, X.-C. (2019). Influences of compaction effect on bearing capacity of laterally loaded piles in sand. *Yantu Gongcheng Xuebao/Chinese Journal of Geotechnical Engineering, 41*, 213–216.

Irawan, C., Djamaluddin, R., Raka, I., & Suprobo, P. (2018). Confinement behavior of spun pile using low amount of spiral reinforcement – An experimental study. *International Journal on Advanced Science Engineering and Information Technology, 8*(2), 501.

Irawan, C., Faimun, F., Putu Raka, I. G., Suprobo, P., Djamaluddin, R., & Soeprapto, G. (2020). Increasing the displacement ductility factor of spun pile using concrete infill. *International Journal on Advanced Science, Engineering and Information Technology, 10*(5), 2028-2034.

Ken't, & Park. (1971). *Flexural Members with Confined Concrete*.

Li, Z., Haigh, S. K., & Bolton, M. D. (2010). The behavior of a single pile under cyclic axial loads. In *GeoShanghai International Conference – Deep Foundations and Geotechnical In Situ Testing* (GSP 205, pp. 143–148). American Society of Civil Engineers.

Owji, R., Habibagahi, G., & Veiskarami, M. (2024). An experimental study on the lateral behavior of piles in unsaturated sand under monotonic, cyclic and post cyclic loading. *Geotechnical and Geological Engineering, 42*(5), 3171–3191.

Quayyum, S. (2010). *Bond behaviour of fibre reinforced polymer (FRP) rebars in concrete* (Master's thesis, Bangladesh University of Engineering & Technology, Bangladesh).

Ren, J., Xu, Q., Chen, G., Yu, X., Gong, S., & Lu, Y. (2022). Full-scale experimental study of the seismic performance of pretensioned spun high-strength concrete piles. *Soil Dynamics and Earthquake Engineering*, 162, Article 107467.

Setiawan, A. F., Darmawan, M. F., Ismanti, S., Sunarso, M., & Adityawarman, G. M. (2020). Numerical model for investigating seismic performance of prestressed hollow concrete (PHC) piles with fiber section element. *E3S Web of Conferences, 156*, 03007.

Setiawan, A. F., Santoso, A. K., Darmawan, M. F., Adi, A. D., & Ismanti, S. (2023). Nonlinear analysis for investigating seismic performance of a spun pile-column of viaduct structure. *Civil Engineering Journal, 9*(7), 1561.